Quantum Electronics **46** (1) 33–38 (2016)

NONLINEAR OPTICAL PHENOMENA DOI: 10.1070/QE2016v046n01ABEH015893

Functional possibilities of nonlinear crystals for frequency conversion: uniaxial crystals

Yu.M. Andreev, Yu.D. Arapov, S.G. Grechin, I.V. Kasyanov, P.P. Nikolaev

Abstract. **The method and results of the analysis of phase-matching and nonlinear properties for all point groups of symmetry of uniaxial crystals that determine their functional possibilities for solving various problems of nonlinear frequency conversion of laser radiation are presented.**

Keywords: *nonlinear optical crystals, frequency conversion, uniaxial crystals.*

The need for laser radiation sources with different wavelengths, intended for various practical applications, has been constantly increasing. The fields of application are laser photochemistry, nonlinear excitation of atoms and molecules, laser photokinetics, ecological monitoring, photobiology, spectroscopy, separation of isotopes, etc. [1–3]. The laser radiation for most of these problems is obtained using the following frequency conversion methods: harmonic generation, sum frequency generation (SFG), difference frequency generation (DFG)] and optical parametric oscillation. The first step in comparative analysis of crystals intended for solving the aforementioned problems is to determine their phase-matching and nonlinear properties in a required wavelength range as necessary and sufficient conditions for frequency conversion. Most of new applications call for repetition of all these procedures, because the wavelength ranges in which phase matching and maximum nonlinear susceptibility coefficient are implemented are usually not determined in the general form for all frequency conversion processes.

Some data on harmonic generation, SFG and DFG at different wavelengths and on the wavelength tuning range for optical parametric oscillators, which were reported in handbook [4], do not make it possible to determine all potential possibilities of crystals in use. At the same time, a traditional problem is to determine the functional possibilities of newly synthesised crystals. The first test experiments on frequency conversion at some fixed wavelength answer only the question about the implementation of phase matching and the value of the effective nonlinear coefficient; however, the complete information about the potential of new crystals for different processes is still to be gained.

In this context, it is necessary to present the information determining the functional possibilities of nonlinear crystals for SFG and DFG in the range of their transparency in the most general form. Here, the first step is to determine the wavelength range in which phase matching and effective nonlinear coefficient $\mathrm{FOM}_1 = d_{\mathrm{eff}}$ (FOM is an abbreviation of figure-of-merit) – the necessary and sufficient conditions for frequency conversion – are implemented. In practice, researchers use generally not FOM_1 but a more informative parameter $\mathrm{FOM}_2 = d_{\mathrm{eff}}^2/n^3$ (n is the refractive index) [5], which characterises the frequency conversion intensity. The results obtained for FOM_2 can be presented as a two-parameter dependence $\mathrm{FOM}_2(\lambda_1, \lambda_2) = d_{\mathrm{eff}}^2(d_{ijk}, \theta_{\mathrm{phm}}(\lambda_1,\lambda_2), \varphi_{\mathrm{opt}})/n^3(\lambda_3)$ (d_{ijk} are the nonlinear susceptibility tensor components), which is calculated along the direction determined by phase-matching angle θ_{phm} (in case of uniaxial crystals, for the optimal polar angle φ_{opt}), for incident radiation wavelengths λ_1 and λ_2, which are related with each other and with wavelength λ_3 by the inequality $\lambda_1 \geqslant \lambda_2 > \lambda_3$. These dependences are given for interactions of all possible types (ooe, oee and eoe for negative crystals and eeo, eoo and oeo for positive crystals).

Typical distributions $\mathrm{FOM}_2 = f(\lambda_1, \lambda_2)$ for a negative KDP crystal belonging to the point group 42m are shown in Fig. 1. Solid curves are isolines for wavelength λ_3, which are obtained for a specified combination of λ_1 and λ_2. Hereinafter, the field beyond the domain of existence of phase matching is given in white for clearness. In view of the above relation for wavelengths λ_1 and λ_2, the distribution is given below the $\lambda_1 = \lambda_2$ line, which corresponds to the second-harmonic generation (SHG). Figure 2 presents the dispersion relations in the conventional form for θ_{phm} and d_{eff} for two types of interaction in KDP crystal. The character of these dependences is in agreement with the data of Fig. 1.

One can select several general properties of the distributions $\mathrm{FOM}_2(\lambda_1, \lambda_2)$, the maxima of which ($\mathrm{FOM}_{2\max}$) determine the ranges of effective frequency conversion. Both in the UV and IR regions, the working range of frequency conversion is limited by either the transparency band of crystal (the most typical situation) or the presence of phase matching. The phase-matching condition for wavelengths λ_1 and λ_2 is always satisfied for the interaction of ooe (eeo) type. This interaction is characterised by the widest wavelength range in which SHG may occur. If the matching condition is satisfied

Yu.M. Andreev Institute of Monitoring of Climatic and Ecological Systems, Siberian Branch, Russian Academy of Sciences, Akademicheskii prosp. 10/3, 634055 Tomsk, Russia; Siberian Physical-Technical Institute, Tomsk State University, Novosobornaya pl. 1, 634050 Tomsk, Russia;
Yu.D. Arapov, I.V. Kasyanov Russian Federal Nuclear Center 'E.I. Zababakhin All-Russian Scientific Research Institute of Technical Physics', ul. Vasil'eva 13, 456770 Snezhinsk, Chelyabinsk region, POB 245, Russia;
S.G. Grechin, P.P. Nikolaev N.E. Bauman State Technical University, Vtoraya Baumanskaya ul. 5, str. 1, 105005 Moscow, Russia; Yaroslavthe-Wise Novgorod State University, Bol'shaya Sankt-Peterburgskaya ul. 41, 173003 Veliky Novgorod, Russia; e-mail: gera@bmstu.ru

Received 1 July 2015; revision received 19 November 2015
Kvantovaya Elektronika **46** (1) 33–38 (2016)
Translated by Yu.P. Sin'kov

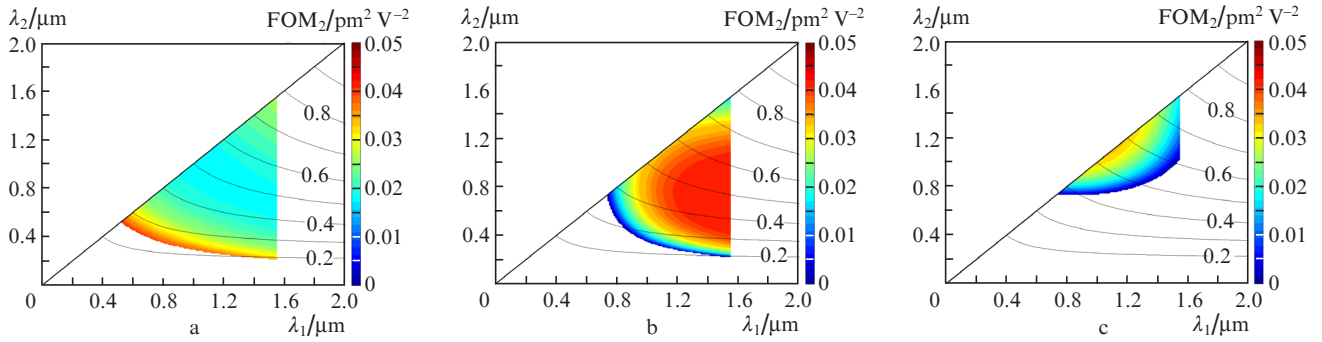

Figure 1. Distributions of the effective nonlinear coefficient of KDP crystal for the (a) ooe, (b) eoe and (c) oee interactions. The numbers on the curves are λ_3 values in μm.

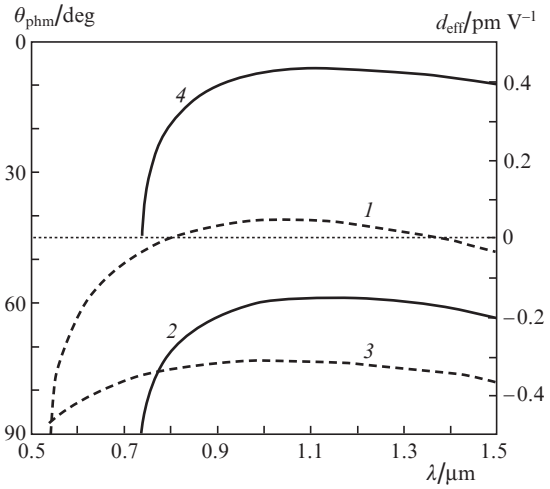

Figure 2. Dispersion relations for (*1*, *2*) θ_{phm} and (*3*, *4*) d_{eff} in KDP crystal under SHG conditions for the (*1*, *3*) ooe and (*2*, *4*) oee interactions.

for this type, the next potentially possible (but not necessarily implemented) type of interaction is eoe (oeo), and the last type in this series is oee (eoo). In the domain of SFG existence, with maximum λ_1 and minimum λ_2 values, the boundaries of FOM_2 distributions are very close (examples are presented in Figs 1a and 1b). However, under these conditions, the range of frequencies λ_3 for the ooe interaction is wider than for the eoe and oee types.

When SHG is implemented ($\lambda_1 = \lambda_2$), the phase-matching wavelength ranges for the eoe and oee interactions coincide; however, the distributions of FOM_2 are generally significantly different for these two types at arbitrary λ_1 and λ_2 values. The character of changes in the distributions $FOM_2(\lambda_1, \lambda_2)$ is determined by the dependence $d_{eff}(\theta)$ and the wavelength dependence of phase-matching angle θ_{phm}. The angular distributions $d_{eff}(\varphi,\theta)$ are identical for the oee and eoe types; however, dispersion relation for θ_{phm} leads to a significant difference between the distributions $FOM_2(\lambda_1, \lambda_2)$ (Figs 1b, 1c).

Our representation of $FOM_2(\lambda_1, \lambda_2)$ clearly indicates that, for example, in a particular case of KDP crystal (Fig. 1), the following types of interaction can be realised: both SHG at $\lambda_1 = \lambda_2 = 0.52$ μm (formation of a wave with $\lambda_3 = 0.26$ μm) and SFG at the transparency edge ($\lambda_1 = 1.55$ μm, $\lambda_2 = 0.22$ μm, $\lambda_3 = 0.19$ μm) at the distribution edges ($FOM_2 > 0$) for the ooe interaction, SFG at $\lambda_1 = 1.55$ μm and $\lambda_2 = 0.6–0.9$ μm ($\lambda_3 = 0.45–0.55$ μm) for the eoe interaction, and SHG in the range of 1.0–1.2 μm ($\lambda_3 = 0.5–0.6$ μm) for the oee interaction. The smallest λ_3 value can be obtained in most cases in the SFG mode rather than under SHG conditions. In the case of KDP crystal, this holds true for both ooe and eoe interactions (Fig. 1). The largest FOM_2 value can be obtained at the frequency conversion edge for the ooe interaction (Fig. 1a), at the transparency edge (Fig. 1b), or in the SHG mode (Fig. 1c).

Obviously, the character of distributions $FOM_2(\lambda_1, \lambda_2)$ is also determined, along with the dispersion relation for refractive indices, by the point symmetry group. The distributions $d_{eff}(\varphi,\theta)$ are generally similar for all crystals belonging to the same point group. This effect is most pronounced for the KDP crystal (point group $\bar{4}2m$) and the crystals isomorphic to it. Some quantitative differences are determined by the dispersion relation for θ_{phm}. There are also some exceptions (see below).

Forty uniaxial nonlinear crystals, belonging to 11 point symmetry groups, are currently used. Some of these crystals are listed in Table 1. The spatial distributions of the effective nonlinear coefficient in crystals representing ten point groups are given in Table 2. Similar distributions for different crystals belonging to the same point group are omitted. Examples of exceptions are BBO and $LiNbO_3$ crystals (point group 3m), characterised by a significant difference in the nonlinear sus-

Table 1. Uniaxial crystals.

Point group	Crystal
$\bar{4}$	HGS ($HgGa_2S_4$)
4mm	LB4 ($Li_2B_4O_7$), Klin ($K_3Li_2Nb_5O_{15}$)
$\bar{4}2m$	ADA ($NH_4H_2AsO_4$), ADP ($NH_4H_2PO_4$), AGS ($AgGaS_2$), AGSe ($AgGaSe_2$), $BeSO_4{\cdot}4H_2O$, CDA (CsH_2AsO_4), $CdGeAs_2$, CLBO ($CsLiB_6O_{10}$), DADA ($NH_4D_2AsO_4$), DADP ($NH_4D_2PO_4$), DCDA (CsD_2AsO_4), DKDA (KD_2AsO_4), DKDP (KD_2PO_4), DRDA (RbD_2AsO_4), DRDP (RbD_2PO_4), KDA (KH_2AsO_4), KDP (KH_2PO_4), RDA (RbH_2AsO_4), RDP (RbH_2PO_4), ZGP ($ZnGeP_2$)
$\bar{6}$	BABF ($BaAlBO_3F_2$)
6mm	CdSe
$\bar{6}$m2	GaSe
6	$LiIO_3$
3m	BBO (β-BaB_2O_4), $LiNbO_3$, $LiTaO_3$, Ag_3AsS_3, Ag_3SbS_3, TAS (Tl_3AsSe_3)
32	KABO ($K_2Al_2B_2O_7$), KBBF ($KBe_2BO_3F_2$), quartz, cinnabar, selenium, tellurium

Table 2. Distributions of $d_{\text{eff}}(\varphi, \theta)$.

Point group (crystal)	ooe	oee, eoe	Point group (crystal)	ooe	oee, eoe
$\bar{4}2m$ (KDP,CLBO)	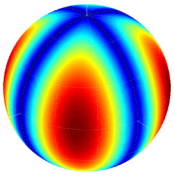	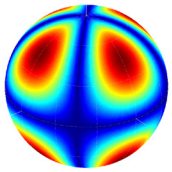	4, 4mm, 6, 6mm (LB4)	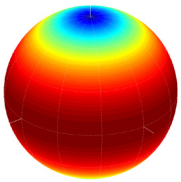	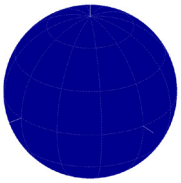
3m (BBO)	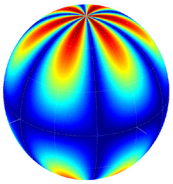	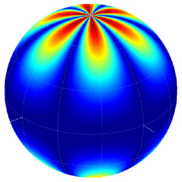	$\bar{4}$ (HGS)	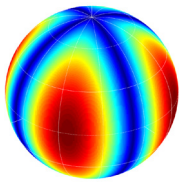	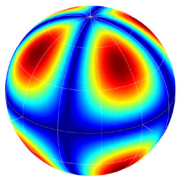
3m ($LiNbO_3$)	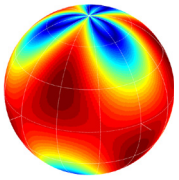	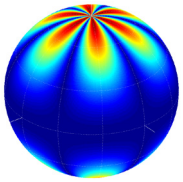	$\bar{6}$m2 (GaSe)	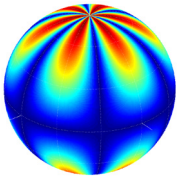	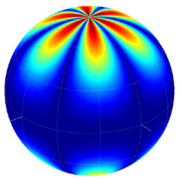
32 (KABO)	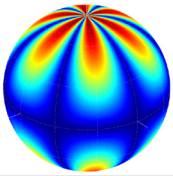	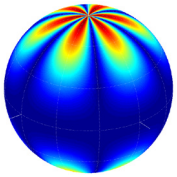	$\bar{6}$ (BABF)	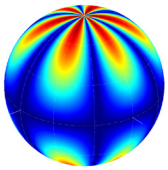	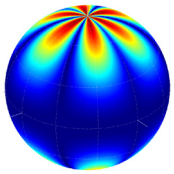

ceptibility tensor components. For example, the tensor component ratio d_{22}/d_{31}, which determines the effective nonlinear coefficient, is 47.2–57.5 for the BBO crystal and 0.48–0.53 for $LiNbO_3$ [4]. This difference is most pronounced for the ooe interaction; however, the distributions for the eoe and oee types are almost identical, because $d_{\text{eff}}(\varphi, \theta)$ is determined by the d_{22} coefficient only [4, 5].

Figure 3 shows the distributions $\text{FOM}_2(\lambda_1, \lambda_2)$ for several crystals. The $\text{FOM}_{2\max}$ values are listed in Table 3.

Table 3. Maximum values $\text{FOM}_{2\max}$ (in $\text{pm}^2\ \text{V}^{-2}$).

Crystal	ooe (eeo)	eoe (eoo)	oee (oeo)
BBO	0.9738	0.7639	0.6567
$LiNbO_3$	2.8584	0.1209	0.0129
LB4	0.004	–	–
Ag_3SbS_3	9.64	9.11	8.93
KDP	0.042	0.043	0.035
CLBO	0.162	0.176	0.176
KABO	0.046	0.034	0.025
KBBF	0.068	0.053	0.045
GaSe	140.2	131.8	127.7
$ZnGeP_2$	154.6	155.7	–
BABF	0.315	0.148	0.121

CLBO and $ZnGeP_2$ crystals (Figs 3a, 3b) belong to the same point group $\bar{4}2m$ as KDP crystal (Fig. 1). The general character of the distribution $\text{FOM}_2(\lambda_1, \lambda_2)$ for the negative CLBO crystal is on the whole similar to that for KDP (the differences are described below). However, for the oee interaction, the wavelength range in which phase matching is implemented is much wider. A significant difference is observed for the positive $ZnGeP_2$ crystal. The reasons are as follows. First, the form of the distributions $d_{\text{eff}}(\varphi, \theta)$ for positive crystals is opposite to that for negative crystals with respect to the interaction types (Table 2). Second, there is a peculiar dispersion relation for the phase-matching angle. As a result, in the case of eoo interaction, phase matching is absent for $ZnGeP_2$ in the entire transparency range of this crystal. The character of the distribution $\text{FOM}_2(\lambda_1, \lambda_2)$ for silver thiogallate (belonging to the same point group $\bar{4}2m$) is on the whole similar to that for KDP crystal.

As was noted above, the distributions $d_{\text{eff}}(\varphi, \theta)$ for the BBO (Fig. 3c) and $LiNbO_3$ (Fig. 3d) crystals (point group 3m) differ significantly in the case of ooe interaction. For $\text{FOM}_2(\lambda_1, \lambda_2)$, this effect manifests itself in the difference in the ranges where its value reaches maximum. This form of $\text{FOM}_2(\lambda_1, \lambda_2)$ for the two aforementioned crystals upon eoe and oee interactions is due to the difference in the dispersion relations for phase-matching angle θ_{phm}. There are specific quantitative differences for Ag_3SbS_3 crystal, which belongs to the same point group (Fig. 3d). For the crystals of point groups 4, 4mm, 6 and 6mm, there is no conversion for oee and eoe interactions, because d_{eff} is zero in this case (Table 2).

Here, we omit the data on mixed compounds (for example, $Hg_yGa_{2-y}S_4$ [6], $AgGa_{1-x}In_xSe_2$, $Hg_{1-x}Cd_xGa_2S_4$ [7, 8], $LiAB_2$ (A = Ga, In; B = S, Se) [9], and $LiGaX_2$ (X = S, Se, Te) [10]), for which the general character of the distributions $\text{FOM}_2(\lambda_1, \lambda_2)$ does not change (as a rule) with some change in the transparency range and the $d_{\text{eff max}}$ value. The same holds true for ADA–DADA, ADP–DADP, CDA–DCDA, KDA–DKDA, KDP–DKDP, RDA–DRDA and RDP–DRDP crystals with different degrees of deuteration.

The sign ratios for tensor components d_{ij} in pyrargyrite crystal have not been exactly known by the beginning of our

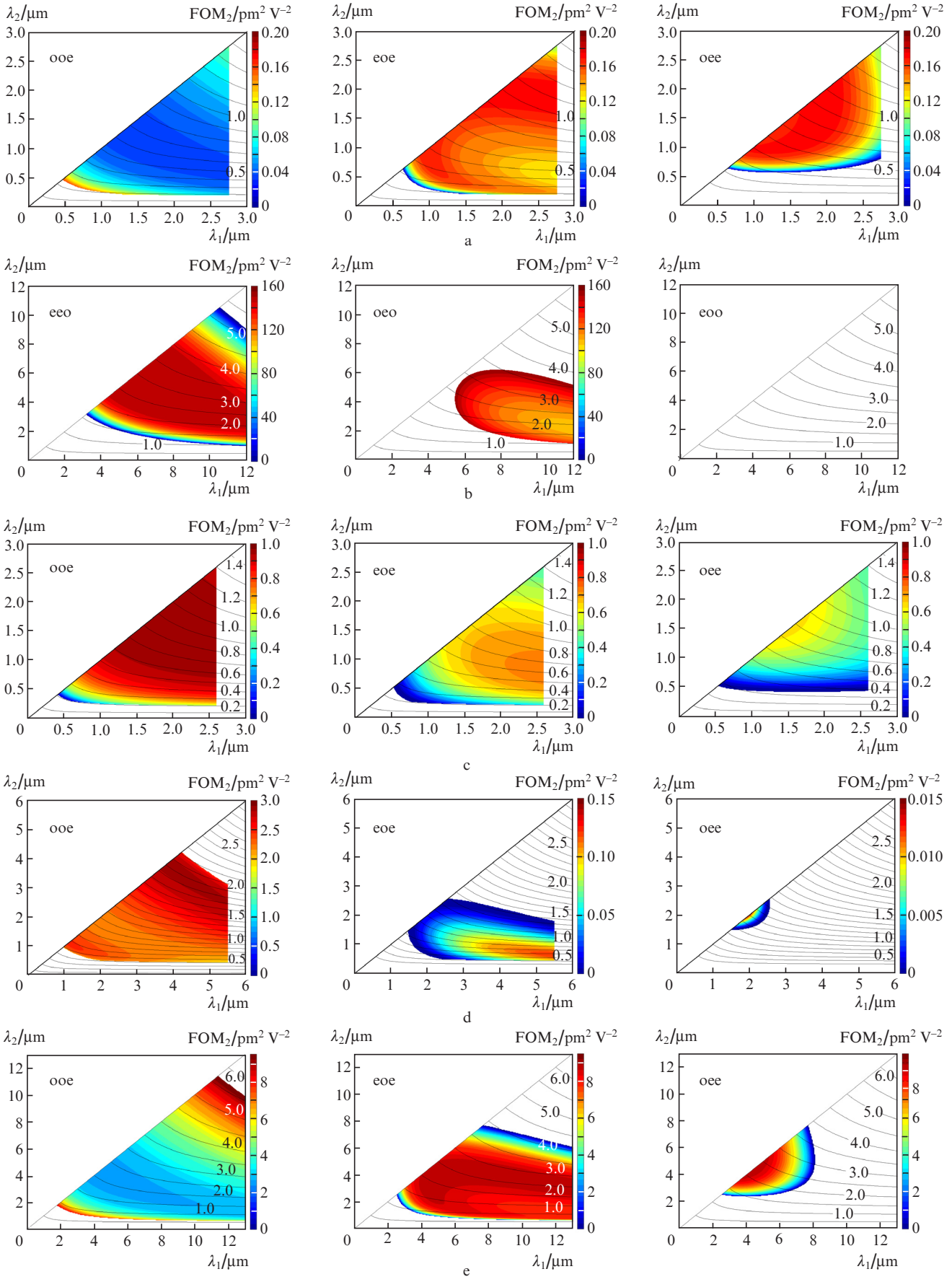

Figure 3. Distributions of FOM_2 for (a) CLBO ($\bar{4}2m$), (b) $ZnGeP_2$($\bar{4}2m$), (c) BBO (3m), (d) $LiNbO_3$ (3m) and (e) Ag_3SbS_3 (3m) crystals upon interactions of different types. The numbers on the curves are λ_3 values in μm.

study. For BABF crystal, we used the following values: d_{11} = 0.165 pm V^{-1} and d_{22} = 1.32 pm V^{-1}, which were reported in [11–13] as a private communication by Ch. Chen.

The dependence $\mathrm{FOM}_2(\lambda_1, \lambda_2)$ makes it possible to determine other important frequency characteristics for all frequency conversion processes. The extremum of the dependence $\theta_{\mathrm{phm}}(\lambda)$ corresponds to the mode of frequency-noncritical phase matching (FNCPM). In this case, wave mismatch for uniaxial crystals in a wide wavelength range is zero ($\Delta k = k_3 - k_2 - k_1 = 0$) and does not change ($\mathrm{d}\Delta k/\mathrm{d}\lambda = 0$, $\mathrm{d}^2\Delta k/\mathrm{d}\lambda^2 \neq 0$); under these conditions, the phase-matching angle θ_{phm} is constant [for example, for KDP crystal (Fig. 2)], as well as the d_{eff} value. The extreme $\mathrm{FOM}_2(\lambda_1, \lambda_2)$ and $\theta_{\mathrm{phm}}(\lambda_1, \lambda_2)$ values are implemented for close λ_1 and λ_2 values. The shift of the extremum of $\mathrm{FOM}_2(\lambda_1, \lambda_2)$ with respect to the extremum of $\theta_{\mathrm{phm}}(\lambda_1, \lambda_2)$ can generally be neglected in most cases in view of the smallness of refractive index dispersion in the problem under consideration. The dispersion of tensor components d_{ijk} is neglected here. Based on this, we can conclude that the $\mathrm{FOM}_2(\lambda_1, \lambda_2)$ value will not change in a wide wavelength range in the FNCPM mode.

However, this is not valid for all point groups. For further consideration, we should note the main features of the wavelength dependences of d_{eff} and θ_{phm} in uniaxial crystals. The dependence $d_{\mathrm{eff}}(\varphi, \theta)$ in most of crystal point groups (Table 2) is monotonic (either decreasing or increasing) in the angular range $0 \leqslant \theta \leqslant \pi/2$. In this case, if there is an extremum in the dispersion relation for θ_{phm}, there must be an extremum in the dependence $d_{\mathrm{eff}}(\varphi, \theta)$ (Fig. 2) and, therefore, in the dependence of FOM_2. In particular, for the ooe interaction in a crystal of point group $\bar{4}2\mathrm{m}$, the existence of extremum can easily be determined by equating to zero the derivative

$$\mathrm{dFOM}_{2\,\mathrm{ooe}}/\mathrm{d}\lambda = -d_{36}\cos\theta_{\mathrm{phm}}\sin(2\varphi_{\mathrm{opt}})\mathrm{d}\theta_{\mathrm{phm}}/\mathrm{d}\lambda.$$

Exceptions are point groups $\bar{4}2\mathrm{m}$, $\bar{4}$ and 3m of $LiNbO_3$ crystal in the case of eoe and oee interactions (Table 2). The FOM_2 extremum for these groups is determined by both the extremum of $d_{\mathrm{eff}}(\lambda)$ and the extremum of $\theta_{\mathrm{phm}}(\lambda)$. For the point group $\bar{4}2\mathrm{m}$ and interactions of eoe and oee types, we have

$$\mathrm{dFOM}_{2\,\mathrm{oee}}/\mathrm{d}\lambda = 2d_{36}\cos(2\theta_{\mathrm{phm}})\cos(2\varphi_{\mathrm{opt}})\mathrm{d}\theta_{\mathrm{phm}}/\mathrm{d}\lambda.$$

Extrema will be observed at $\theta_{\mathrm{phm}} = \pi/2$ and $\mathrm{d}\theta_{\mathrm{phm}}/\mathrm{d}\lambda = 0$. If $\pi/2 \leqslant \theta_{\mathrm{phm}} < \pi/4$, the character of the dependence is determined by only the extremum of θ_{phm}. In this range of θ_{phm} angles, phase matching occurs for the overwhelming majority of crystals belonging to the aforementioned point groups. However, in a particular case of CLBO crystal and oee interaction under SHG conditions (Fig. 4), phase matching occurs also at $\theta_{\mathrm{phm}} > 45°$. The minimum in the central part of the dependence $d_{\mathrm{eff}}(\lambda)$ corresponds to the maximum of $\theta_{\mathrm{phm}}(\lambda)$, and the two maxima correspond to the maximum values of d_{eff}.

Thus, the results presented in Fig. 3 can be used to determine the combinations of wavelengths λ_1 and λ_2 at which FNCPM is implemented. Under the SFG conditions, the question about the necessity of FNCPM is urgent in two cases:

(i) frequency conversion for an ultra-short laser pulse (USLP) at one of the input radiation wavelengths (λ_1 or λ_2) and for a quasi-steady-state pulse at the other wavelength (λ_2 or λ_1); and

(ii) frequency conversion for two USLPs at λ_1 and λ_2.

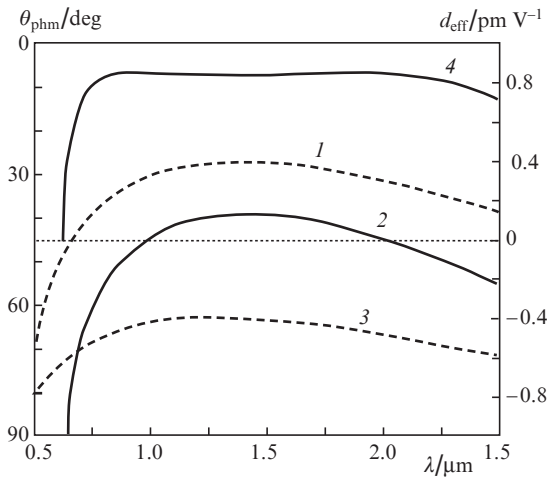

Figure 4. Dispersion relations for (*1*, *2*) θ_{phm} and (*3*, *4*) d_{eff} in CLBO crystal under SHG conditions: (*1*, *3*) ooe and (*2*, *4*) oee interactions.

In the former case, one considers the allowable wave mismatch between a USLP with a wavelength λ_1 or λ_2 and a newly formed wave with λ_3. In the latter case, the pairwise interaction between both waves with λ_1 and λ_2 and the wave with λ_3 is considered. Here, as in the case of conventional determination of phase-matching widths, processes occurring with plane monochromatic waves are analysed. The allowable wave mismatch is determined for the extreme frequencies of pulse spectra.

Let us now determine the conditions for implementing these modes by an example of BBO crystal upon eoe interaction (Fig. 5). FNCPM may occur in the former case if the tangent to the FOM_2 isoline is parallel to either λ_1 or λ_2 axis. In this case, the FOM_2 value remains constant in a wide range of variation in λ and, therefore, the angle θ_{phm} does not change. One of particular cases is shown in Fig. 5. For example, for point A (λ_1 = 1.46 μm and λ_2 = 1.13 μm), $\mathrm{dFOM}_2/\mathrm{d}\lambda_1 = 0$; this equality determines the possibility of SFG for a USLP with a wavelength λ_2 and a long pulse with λ_1. For point B (λ_1 = 2.17 μm and λ_2 = 1.63 μm), $\mathrm{dFOM}_2/\mathrm{d}\lambda_2 = 0$. Here, FNCPM may occur for a USLP with λ_1 and quasi-steady-state radiation with λ_2.

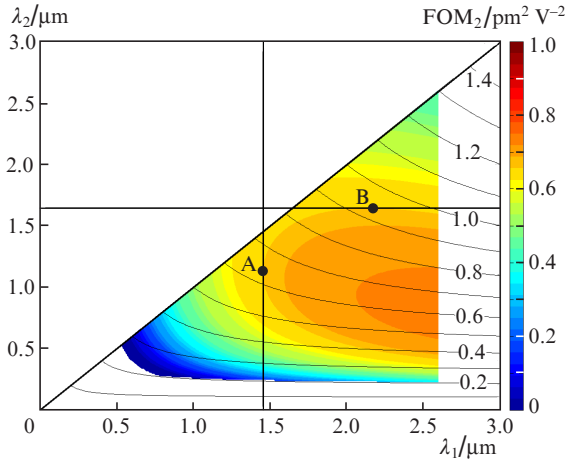

Figure 5. Distributions of FOM_2 in BBO crystal upon eoe interaction. The numbers on the curves are λ_3 values in μm.

A general analysis of the dependences in Fig. 5 shows that the FNCPM mode for USLPs with wavelengths of λ_1 and λ_2 can be implemented, respectively, in the ranges of $\lambda_1 = 1.18-2.6$ μm and $\lambda_2 = 0.87-2.0$ μm. Having chosen a point on the FOM_2 isoline, one can set a desired ratio of spectral widths of pulses with λ_1 and λ_2 (pulse durations) to make the frequency conversion most efficient.

To confirm the general character of the dependences under consideration, Fig. 6 presents the tuning characteristics for BBO crystal in a conventional form. The dependences $\lambda_1(\lambda_3)$ at a fixed θ value have extrema (indicated by circles in the curves). The λ_1 value remains invariable in the vicinity of these extrema in a fairly wide range of variation in λ_3, while λ_2 changes linearly. This behaviour occurs at different λ_3 values, which are determined by angle θ.

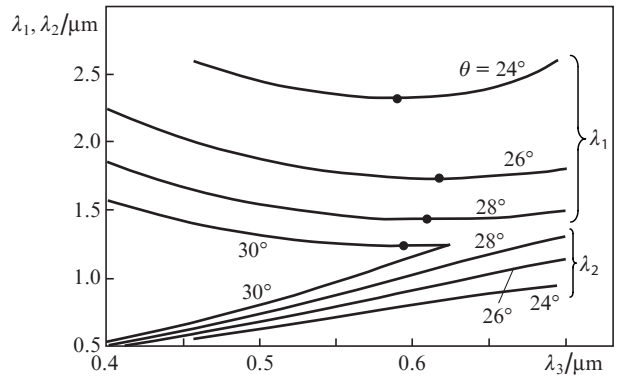

Figure 6. Tuning characteristics for BBO crystal (eoe interaction).

It follows from Figs 1 and 3 that SFG for two waves, one of which is narrowband and the other is broadband, may occur in KDP (eoe), CLBO (eoe, oee) (at some wavelength ratios), $ZnGeP_2$ (oeo), BBO (eoe), $LiNbO_3$ (eoe) and Ag_3SbS_3 (eoe) crystals. SFG may also occur for two waves with λ_1 and λ_2 and a broad spectrum.

Similarly, Figs 1 and 3 yield information about the potential characteristics of crystals in the case of parametric generation of light as a problem inverse to SFG. At a specified λ_3 value, one can determine desired ranges of wavelengths λ_1 and λ_2 for interactions of different types. One can also estimate the possibility of forming radiation with different spectral widths (by analogy, for example, with Fig. 5) and the ratio of spectral widths of both waves. The rate of variation in FOM_2 is related to the range of variation in angle θ for implementing conversion with respect to wavelengths λ_1 and λ_2.

The existence of tangents to FOM_2 isolines (Fig. 5), for example, for KDP (ooe), CLBO (eoe), $ZnGeP_2$ (oeo), BBO (ooe, oee), $LiNbO_3$ (ooe, eoe) and Ag_2SbS_2 (ooe, eoe) crystals, characterises the conditions under which a broadband beam with a wavelength λ_1 or λ_2 is formed (under narrowband pumping at λ_3) in the direction determined by angle θ. In the case of DFG, there is a possibility of forming and amplifying a pulse with a wide spectrum (for example, a femtosecond pulse) in the field of narrow-band radiation with λ_3. There may also be an inverse situation: formation of narrow-band radiation at λ_1 or λ_2 under broadband pumping at a wavelength of λ_3 (points A or B, respectively, in Fig. 5).

To perform a simple analysis of the possibility of implementing DFG in different crystals, FOM_2 distributions can be presented as functions of wavelengths λ_1 and λ_3 [$FOM_2(\lambda_1, \lambda_3)$] or λ_2 and λ_3 [$FOM_2(\lambda_2, \lambda_3)$].

Thus, the method proposed here to describe frequency characteristics and represent results is a convenient and descriptive reference technique for determining the functional possibilities of crystals in frequency conversion problems and for carrying out their comparative analysis when solving various applied problems. The results of this study show the possibility of determining frequency characteristics for various processes.

Acknowledgements. We are grateful to E.V. Yugova for her help in different stages of the study.

This work was supported by the Russian Foundation for Basic Research (Grant No. 15-02-07760); Siberian Branch of the Russian Academy of Sciences (Project VIII.80.2.4); Tomsk State University (Grant No. 8.1.51.2015); and Russian Science Foundation (in the part concerning the development of the technique for analysing and processing results by S.G. Grechin and P.P. Nikolaev) (Grant No. 15-11-10023).

References

1. Letokhov V.S. *Lazernaya fotoionizatsionnaya spektroskopiya* (Laser Photoionisation Spectroscopy) (Moscow: Nauka, 1987) p. 319.
2. Letokhov V.S. *Laser Control of Atoms and Molecules* (Oxford University Press, 2007) p. 320.
3. Hannaford P. (Ed.) *Femtosecond Laser Spectroscopy* (Boston: Springer Science & Business Media, 2005) p. 350.
4. Dmitriev V.G., Gurzadyan G.G., Nikogosyan D.N. *Handbook of Nonlinear Optical Crystals* (Berlin: Springer, 1999).
5. Dmitriev V.G., Tarasov L.V. *Prikladnaya nelineinaya optika* (Applied Nonlinear Optics) (Moscow: Fizmatlit, 2004).
6. Wang T.-J., Kang Zh.-H., Zhang H.-Zh., Feng Zh.-Sh., Wu F.-G., Zang H.-Y., Jiang Y., Gao J.-Y., Andreev Y., Lanskii G., Atuchin V., Parasyuk O. *Appl. Phys. Lett*., **90**, 1913 (2007).
7. Ji G., Shen T., Huang J., Zhao B., Andreev Yu.M., Atuchin V.V., Lanskiy G. *Proc. SPIE Int. Soc. Opt. Eng*., **6595**, 659514 (2007).
8. Petrov V., Rotermund F., Badikov V.V., Shevyrdyaeva G.S. *Proc. Conf. on Lasers and Electro-Optics (CLEO'03)* (Baltimore, 2003) p. CMA5.
9. Petrov V., Noack F., Isaenko L., Yelisseyev A., Lobanov S., Titov A., Rotermund F., Zondy J.-J. *Proc. Conf. on Lasers and Electro-Optics (CLEO'03)* (Baltimore, 2003, CTuN5) pp 733–734.
10. Isaenko L., Yelisseyev A., Lobanov S., Titov A., Krinitsin P., Petrov V., Zondy J.-J. *Proc. Conf. on Lasers and Electro-Optics (CLEO'03)* (Baltimore, 2003, CWA15) pp 1000–1001.
11. Yoshimura M., Mori Y., Hu Z.G., Sasaki T. *Opt. Mater*., **26**, 421 (2004).
12. Zhou Y., Wang G., Yue Y., Li Ch., Lu Y., Cui D., Hu Zh., Xu Z. *Opt. Lett*., **34**, 746 (2009).
13. Zhou Y., Yue Y., Wang J., Yang F., Cheng X., Cui D., Peng Q., Hu Zh., Xu Z. *Opt. Express*, **17**, 20033 (2009).